JOURNAL OF AIRCRAFT
Vol. 41, No. 2, March–April 2004

Corrosion Fatigue in 7075-T6 Aluminum: Life Prediction Issues for Carrier-Based Operations

Basir Shafiq*
University of Puerto Rico, Mayagüez, Puerto Rico 00681
and
Vinod S. Agarwala†
U.S. Naval Air Systems Command, Patuxent River, Maryland 20670

Fatigue experiments performed on 7075-T6 Al alloy at various frequencies and stress levels and under alternating wet and dry environments indicate that simultaneous action of corrosion and fatigue substantially accelerates crack initiation and growth rates when compared to pure fatigue (dry air) conditions. In experiments performed under alternating wet and dry conditions, fatigue crack growth rate was observed to increase rapidly in the presence of mildly corrosive (salt solution) and decrease sharply when subjected to noncorrosive dry air. Crack arrest of various durations was observed at transition points between dry and wet cycles. Lowering the frequency of fatigue loading significantly reduced crack initiation and overall life time. S-N curves showed a continuous downward trend without reaching a plateau or threshold. These observations led to the conclusion that aircraft structural integrity can be seriously compromised even under mildly aggressive environments and at subcritical stress levels when cracks are present regardless of changing of environments and/or test frequency.

Nomenclature

a	=	crack length
i_a	=	crack tip current density
N	=	number of cycles
R	=	stress level ($\sigma_{\min}/\sigma_{\max}$)
t	=	time
w	=	specimen depth (distance from the notch tip to the end of the specimen in the direction of the crack growth)
ΔK	=	change in stress intensity factor
δ	=	crack opening displacement
$\delta_{\max}$	=	crack opening displacement corresponding to $\sigma_{\max}$
$\delta_{\min}$	=	crack opening displacement corresponding to $\sigma_{\min}$
δ_r	=	ratio of $\delta_{\max}/\delta_{\min}$

Introduction

SEVERITY of service environment has forced the U.S. Navy to adopt a safe-life policy in determining the lifetime of aircraft metallic structures. Because the U.S. Navy has a large inventory of aging aircraft, the concerns related to the remaining life of aircraft are highly dependent on structural integrity issues. It is also a fact that material degradation due to effects of corrosion and fatigue can pose a serious threat to mission readiness and reliability. Under the conjoint action of mechanical fatigue and corrosion, the mechanisms of structural failure become highly complex, and simple models, which relate to pure fatigue or electrochemical actions or simple superposition of the two, do not apply.[1] A comprehensive corrosion fatigue crack growth (CFCG) model is yet to appear that can accurately predict lifetime (stages for crack initiation and propagation) of aircraft structures. The primary difficulty appears to be the lack of experimental techniques/tools that are required to quantify crack tip electrochemical/micromechanical (E/M) parameters, such as corrosion current density, hydrogen generation and absorption, microcracking, etc.

Most mechanistic models treat time as an independent variable, but corrosion is a time-dependent phenomenon. Hence, aging or the effects of time (loading frequency and stress) on fatigue crack growth due to corrosion are significant: The kinetics of the (electrochemical) reactions occurring at the crack tip are immensely accelerated under stress and low-frequency cyclic action.[2–6] Because aircraft structures invariably go through various cycles of chemical and thermal environments throughout their life, it is, therefore, of interest to study the effects of changing environment on the overall life of the structure. However, the literature available on this subject is scarce. An unsuspected activity associated with changing environments is the crack closure phenomena because severe crack arrest has been observed in metals subject to environmental changes during fatigue lifetime especially at low crack driving forces, ΔK, δ, R, etc.[7,8] Several other parameters simultaneously take part in CFCG, such as metal dissolution (MD), hydrogen embrittlement (HE), microcracking, grain size, toughness, type of environment, and multisite interactions, to name a few.[1] Needless to say, it is rather difficult to study all of these parameters simultaneously. A good experimental strategy would be to decouple the parameters and understand how various crack tip E/M parameters interact with each other. This could be crucial in the development of accurate lifetime prediction methodology. Therefore, in this study experiments have been conducted to characterize CFCG behavior of the commonly used aircraft structural alloy 7075-T6-Al in a mildly aggressive (salt solution) environment as a function of frequency, stress, and alternating crack tip environmental conditions. Some mathematical models have been proposed and their limitations discussed.

Experimental Setup

It has been shown[6] that in the presence of chloride ions the pH of crack tip can be acidic even when the bulk solution is almost neutral. This occurs due to the hydrolysis of corroding species such as aluminum. Because the pH of the naval (service) environment can vary anywhere between 3 and 5, a mild 1%NaCl solution of pH $\sim$ 2.5 (simulating crack tip pH) was selected for CFCG testing. Preliminary testing was done to study free corrosion kinetics. All tests were performed at room temperature. Quasi-static tests were initially conducted to obtain ultimate static strength of compact tension (CT) specimens, which was on the average of 17 kN. Subsequently fatigue testing was performed on standard CT specimens.

Received 21 November 2001; revision received 24 March 2003; accepted for publication 10 June 2003.

*Associate Professor, Department of General Engineering, Box 9044; a_basir@rumac.uprm.edu.

†Senior Scientists, Research and Engineering Group, 48110 Shaw Road Unit 5; agarwalavs@navair.navy.mil.

To study the effects of precorrosion, crack tip subject to corrosive solution (ACT)/crack tip subject to dry air conditions (ICT), and loading frequency on the crack growth rate (CGR) characteristics, testing was performed at a constant load (equal to 972 N, about 5.5% of the ultimate static load) and $R = 0.1$, while the loading frequency was varied from 1 to 30 Hz. Tests under various stress levels (7–18% of the ultimate static load) and three different frequencies (0.2–1.0 Hz) were performed to study the effect of frequency on S-N behavior of the material under ACT conditions. To study CFCG under alternating crack tip environments, two sets of tests were performed at a constant loading frequency (1 Hz): one at a constant $K = 6.6$ MPa $\cdot$ m$^{1/2}$ and $R = 0.1$ and 0.4 and the second one at a constant load of 1335 N (about 8% of the ultimate static load) and $R = 0.4$. Additional tests were also performed under ACT and ICT conditions to obtain baseline data for each set of testing parameters (load, Δk, R, ν, etc.). Crack initiation (taken equal to 0.25 mm) was carried out under ACT conditions, except for the specimens tested under ICT, which were precracked according to the American Society for Testing and Materials E399-95 standard. Crack length was calculated using a compliance technique, but it failed to yield physically acceptable results during crack-closure stage of testing, where optical means were employed to obtain accurate crack length measurements.

Loading and Environmental Effect

Effect of Precorrosion

Irrespective of the extent of precorrosion at any loading frequency, test results indicated a sharp decrease in the crack initiation time under ACT conditions revealing severe effects of environment on the material deterioration and cracking under stress. The results of ACT and ICT on CFCG behavior beyond crack initiation suggested that the effects of precorrosion do not contribute in the ensuing fatigue CGR. Figure 1 shows the independence of CGR on the precorrosion time by comparing specimens tested after being subjected to 5 and 12 days of precorrosion.

Effect of Frequency

To study the effect of frequency (time) on CFCG, specimen crack tips were kept active during testing. Figure 2 shows the dramatic difference in CFCG rates of specimens tested in ICT/ACT conditions and subjected to various frequencies. Increasing frequency (from 1 to 30 Hz) increased the fatigue life in ACT specimens reaching a threshold at around 10 Hz, beyond which further increase in life was not significant. Lifetime in ICT specimens was found to be independent of frequency. ACT specimens exhibited an up to fivefold increase in the CGR at all frequencies, leading to significantly reduced lifetime in the crack propagation stage as compared to precracked ICT specimens. The total lifetime under ICT would be substantially higher because crack initiation time consumes most of the material's life. An increase in the CFCG at a lower loading frequency is associated with longer time per cycle for electrochemical reactions to occur such as ionic transport, anodic dissolution, and hydrogen diffusion and embrittlement. Figure 2 indicates that the CFCG rate decreases as the loading frequency is increased. However, it never approaches the CGR of ICT specimens, indicating the presence of corrosion effects even at very high frequencies (or short times). It appears that the difference in the CGRs at various frequencies grows as the crack grows longer and ΔK increases. However, the trend remains unchanged at the earlier stages of CGR as indicated by the Fig. 2 inset. At earlier stages of CGR when the stress intensity factor is below threshold, the crack tip plasticity-induced crack closure process can complicate the CFCG phenomena. Crack closure is discussed in more detail in the alternating environment section.

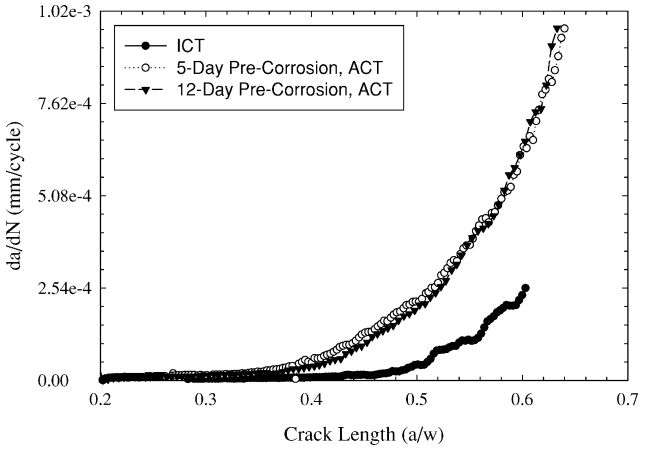

Fig. 1 CFCG test results under ACT and ICT conditions and at two different precorrosion times; significant jump in fatigue CGR is observed in the case of ACT condition.

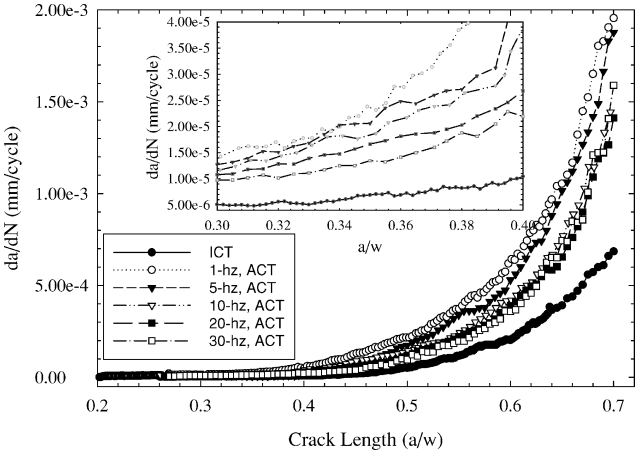

Fig. 2 Comparison of fatigue CGR results for tests conducted at different frequencies under a constant load condition.

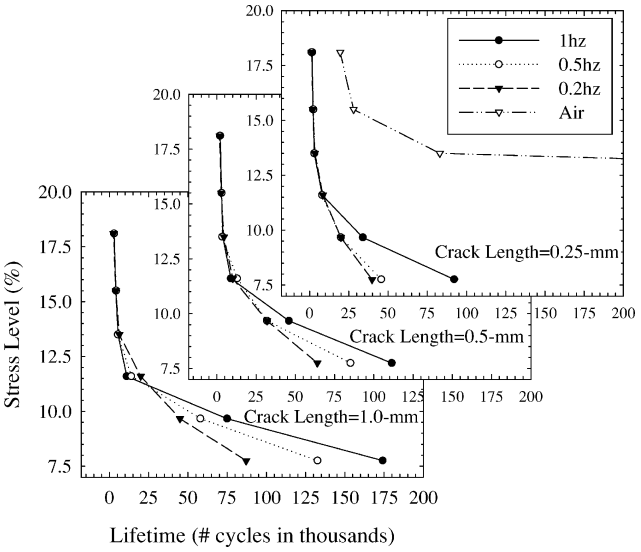

Fig. 3 ACT and ICT S-N curves at various crack lengths and frequencies.

Effect of Stress

S-N curves provide a useful indication of the remaining life of the material and can be subsequently used in a predictive lifetime model. S-N tests were performed at low stress levels (between 7 and 18% of the ultimate static strength) to obtain life as defined by the U.S. Navy's safe-life policy, that is, reaching a crack length of 0.25 mm. S-N curves in an ICT environment typically yield an increased lifetime as the stress level is reduced, reaching a plateau at some stress below which an infinite life is generally assumed. Figure 3 shows an up to one order of magnitude reduction in lifetime

(of 0.25-mm crack length) in ACT specimens as compared to ICT specimens. ICT specimens reached an infinite life below 13% stress level (test terminated at 500,000 cycles) mainly because crack initiation never took place. However, an infinite life is never obtained, and instead, a continuous downward trend is observed in the S-N curves of the material subject to ACT environments, as shown in Figs. 3 and 4. Furthermore, under ICT conditions, lifetime is independent over a wide range of frequencies. However, because corrosion is a time-dependent phenomenon, the S-N curves of CFCG strongly depend on the loading frequency. Hence, Fig. 4 shows a significant reduction in corrosion fatigue life as the frequency is reduced from 1 to 0.2 Hz.

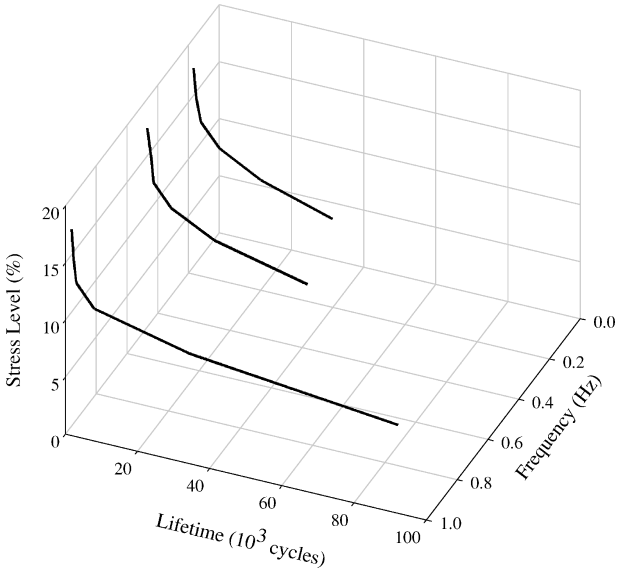

Fig. 4 Three-dimensional plot of stress level (7–18%), frequency (1–30 Hz), and lifetime.

The U.S. Navy's current safe-life policy dictates a crack length tolerance of no more than 0.25 mm, whereas a damage tolerant design can, in principle, allow the crack to grow to a significant length beyond safe life limit. Comparisons of specimen lifetimes shown in Fig. 3 indicate an up to 50% increase in life during each increment of 0.25-mm crack length. Utilization of this additional lifetime can translate into significant savings of revenue in terms of parts and maintenance.

Discussion

The observed increase in CFCG may be explained in terms of various E/M processes simultaneously taking place at the crack tip, such as MD, HE, crack tip microcracking,[1,6,9] etc. In the MD process, potential differences are created between distinct anodic and cathodic sites at high- and low-stress points, respectively. The crack tip that is smallest in area and highest in stress becomes an anode and develops a very high-current density, thus accelerating the dissolution of the crack tip. In an open-circuit system, anodes and cathodes with small potential differences and area ratios result in much lower corrosion current density. At the crack tip under corrosion-assisted fatigue stresses, the CGRs are, therefore, significantly higher.[1,6]

Diffusion of hydrogen and formation of hydrides may occur simultaneously at the crack tip, which causes critical stress intensity to decrease, allowing the crack to propagate into the brittle hydride phase. In addition, the chemical potential of solute hydrogen and hydrides is reduced at tensile stress conditions such as crack tips. The greatly decreased stress intensity factor and reduced chemical potential allow rapid crack propagation when the applied stress is only moderately increased.[1,4,6] Furthermore, as a material fatigues, it develops a zone of microcracks, which is formed in the vicinity of the crack tip. This facilitates diffusion of salt-laden moisture and acid (H^+ ions) at the crack tip, which in turn accelerate MD and HE processes. Depending upon the material, the state of stress and frequency, etc., the microcracking zone size may be quite significant and, consequently, needs to be accounted for in analysis.

The surface morphology of cracked specimens showed severe effects of corrosion. The specimens tested under ICT conditions showed typical intragranular failure features (Fig. 5a), whereas the

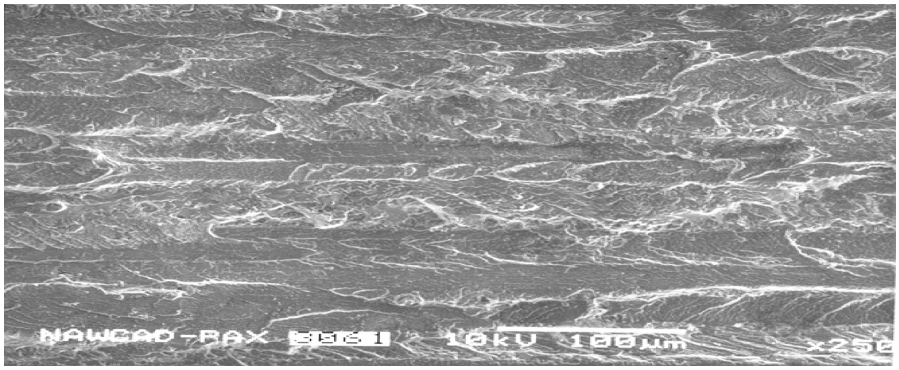

Fig. 5a Surface morphology of cracked specimen tested under ICT condition; typical surface roughness of ductile failure is observed.

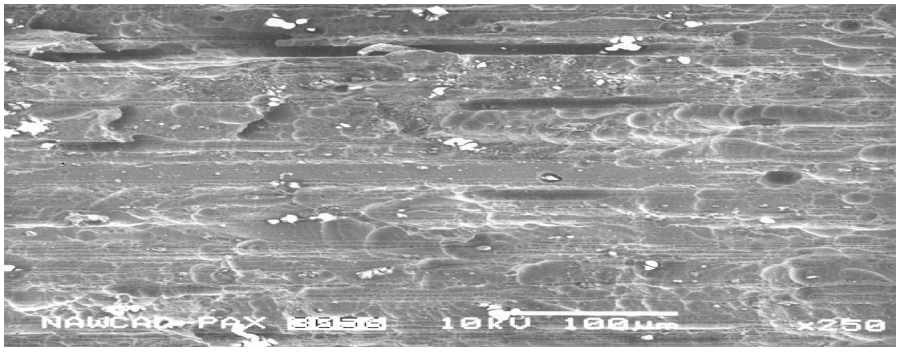

Fig. 5b Surface morphology of cracked specimens tested under ACT condition; smoother surface with crevices and holes is observed.

ACT specimens exhibited a intergranular failure (Fig. 5b) reflected by smoother cracked surface with pits and crevices, a typical feature of corroded surface. However, scanning electron microscope (SEM) evidence obtained in this case was not sufficient to isolate various crack tip E/M processes. It is generally accepted that the predominant environmental crack growth mechanism in high-strength Al alloys is HE.[1,6,10–12] SEM results strongly hint at MD having an active role in the overall crack growth behavior. Figure 5b shows a grain boundary dissolution and subsequent failure along the grain boundaries causing smooth crevices. Furthermore, considerably smaller closing strains, δ_{min}, were obtained under ACT conditions, a behavior that generally speeds up the CGR and indicates the presence of MD, as discussed in detail in the following section. SEM results lead to at least a strong possibility that CFCG behavior in 7075-T6 Al is also shared by the MD process, in addition to HE.

The results presented in this section related to the effects of precorrosion, frequency, and stress level strongly indicate that a mildly aggressive salt solution environment, even at sub-critical fatigue stresses, can significantly raise CFCG rates and impose its detrimental effects on aircraft structures.

Effects of Alternating Environment/Crack Arrest

An operational aircraft structure is invariably exposed to varying humidity, temperature, and chemical environments. Test results described in the preceding section (Figs. 2–4) revealed detrimental effects of corrosive environment on the crack initiation and growth mechanism. To gain further understanding of how a changing environment may affect the actual fatigue life of an aircraft, alternating ACT/ICT cycle tests were conducted. The first test was performed at a constant load of 5.5% (of ultimate static load) at $R = 0.1$. Environments were altered at regular crack length and/or time intervals. Under stable conditions, CGR followed the behavior of its respective environment (ACT or ICT). However, severe crack closure was observed especially at ICT to ACT transition points, sometimes leading to a complete crack arrest. Because of crack arrest, this test proved to be extremely time consuming and was terminated after three cycles. Crack arrest phenomenon was attributed to the sudden change in δ_{min} (the closing δ), R, and ΔK.

To reduce the effects of transition point crack arrest, the R ratio was increased to 0.4 to raise δ_{min}, and the constant load was increased to 8% (of the ultimate static load) to raise ΔK. Moderate crack arrest was still observed especially at lower ΔK values, that is, at earlier stages of the test. Crack driving mechanisms not only depend on the applied stress level but also on the relative crack tip strain, that is, the ratio of $\delta_r (= \delta_{max}/\delta_{min})$; lowering the δ_r lowers the crack driving force. Test results indicate that the crack arrest was more severe going from ICT to ACT conditions as δ_r decreased due to sudden and temporary increase in δ_{min}. Whereas during ACT to ICT transition, hardly any crack arrest was noticed because no significant change in δ_r took place.

It is well-known that a tension/compression condition is more severe than tension/tension condition at the crack tip.[13] This idea can be extended to contend that the ratio of $\sigma_{max}/\sigma_{min}$ (proportional to $\delta_r = \delta_{max}/\delta_{min}$) would have a similar effect on the CGR. A higher δ_r ratio would be more severe at the crack tip than a lower one. Thus, during the transition from the ICT to ACT cycle, with solution at the crack tip, δ_{min}, increases (reducing δ_r) whereas the compression effects decrease at the crack tip, which tends to slow down the crack growth. Furthermore, under ICT conditions, the intragranular failure-induced roughness does not allow the crack to close perfectly. However, during the ACT cycle the corrosive solution dissolves grain boundaries, thus, dislodging surface grains that were subjected to intragranular failure during the ICT cycle. As a result, the surface in the vicinity of the crack tip smoothens, leading to a decrease in δ_{min} (and, consequently, an increase in δ_r), resulting in enhanced crack driving forces at the crack tip. The increase in CGR is also aided by the corrosion (MD and HE) at the crack tip, which is a very rapid process. A schematic of crack/notch profile of the process occurring during the ACT/ICT transition periods is shown in Fig. 6.

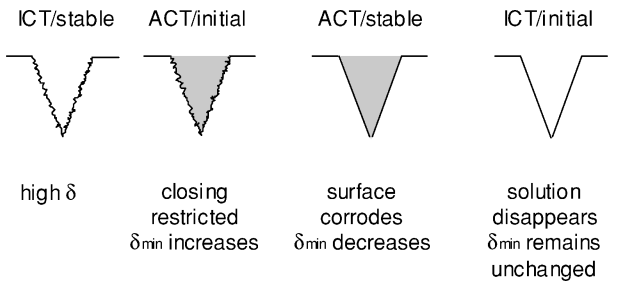

Fig. 6 Schematic of the effect of changing environment at the notch/crack tip.

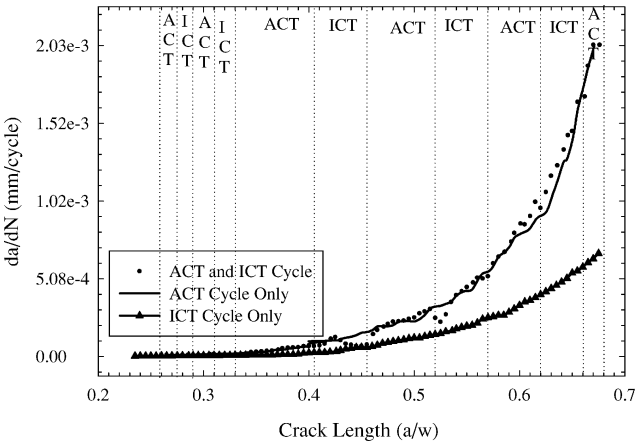

Fig. 7a Fatigue CGRs in alternating ACT and ICT conditions under constant load testing.

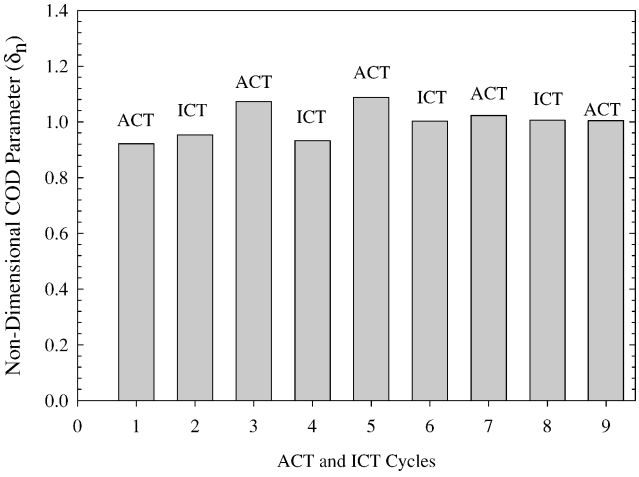

Fig. 7b Nondimensional δ_n values obtained from alternating ACT and ICT environment test conducted under constant load.

Dissolution of the crack surfaces and reduction of δ_{min} in the ACT conditions is a further indication of the presence of MD process in the overall crack growth mechanism. As shown in Fig. 5, crack surface morphology cannot be smoothed (to reduce δ_{min}) by the effects of HE; this phenomena is unmistakably due to MD.

It was observed during the load-controlled testing that crack arrest was either nonexistent or comparatively short going from ACT to ICT conditions at both load levels (5.5%/0.1R and 8%/0.4R). Stable ACT conditions (beyond transition point) give rise to a higher δ_r, as already discussed. When the solution is suddenly sucked out of the crack area during the transition to the ICT cycle, δ_{min} experiences a negligible decrease, thus, leaving δ_r virtually unaffected, that is, no crack arrest. However, ICT environmental conditions rapidly take over crack growth kinetics, thus, reducing CGR. In time, δ_{min} increases due to crack surface roughness, etc., thus further reducing the crack driving forces. Figure 7a shows the variation in the CGR

under ICT and ACT environments. CGR is more sensitive to changing environment while in the low ΔK regime, as shown in Fig. 7a. To further accentuate the role δ_r plays in the crack arrest mechanism, a nondimensional form of δ_n was obtained as

$$\delta_n = (\delta_{\max}/\delta_{\min})(\delta_{\text{final}}/\delta_{\text{initial}}) \tag{1}$$

and is shown in Fig. 7b. Note from Fig. 7b that during the stable crack growth regime, the ICT cycle $\delta_{n/\text{ICT}}$ is lower than the ACT cycle $\delta_{n/\text{ACT}}$. However, this effect disappears at higher ΔK values.

A constant-load test hinted at the ΔK dependence of CGR, as observed from Fig. 7a. To understand alternating environment and crack arrest phenomena better, a constant K test was performed at 6.6 MPa $\cdot$ m$^{1/2}$ and $0.4R$. Figure 8a shows the sharp differences in the crack growth behavior during ACT and ICT environments. Note from Fig. 8a that at the later stages of crack growth substantial load decreases to maintain constant K causes the crack tip strains to drop significantly to have virtually a crack arrest during the ICT cycle. However, at the same low subcritical crack tip strain, a change in environment to the ACT condition sped up the crack growth due to corrosion occurring at the crack tip.

The crack arrest mechanism at ICT to ACT transition points is slightly more enhanced in this case because the CGRs were fairly constant under constant ΔK. Figure 8b shows the actual $\delta_{\max}$ and $\delta_{\min}$ and crack arrest durations at transition points for this test. Once again, during ACT to ICT transition, insignificant crack arrest was observed. However, ICT to ACT crack arrest durations showed an increase as the crack grew longer. This occurred as a result of lower effective crack driving forces (ΔK and δ_r), a conclusion followed from the preceding discussion and observations made from Fig. 8c, where δ_n values at ICT cycle are consistently lower than the ones obtained during the ACT cycle throughout the testing. Note that the difference in δ_n during ACT and ICT cycles increased as the crack grew longer, thus, relating this parameter to the corrosion fatigue crack driving mechanism.

Prediction Methodologies

Because CFCG is influenced by several simultaneously acting but mostly unquantifiable factors, a useful/comprehensive predictive model seems unlikely. Many CFCG mathematical models, each with its own limitations and criticisms,[1] have been reported in the literature.[10–17] A stumbling block in modeling appears to be an experimental setup that could yield quantitative values of various E/M activities occurring in the vicinity of the advancing crack tip. A versatile lifetime prediction methodology of relevance that relates CGR to crack tip E/M mechanisms is needed to better estimate the effects of corrosion on the lifetime of the aircraft structures. Perhaps such a model could become the basis of a review of U.S. Navy's strict safe-life policies. Here a brief discussion of some basic methodologies and techniques that can be useful in formulating the crack growth models is presented.

Superposition of corrosion-induced crack growth and mechanical fatigue crack growth represents the most common approach in developing CFCG modeling,[1,14] which can be described by the following competing mechanisms:

$$\frac{da}{dt_{\text{total}}} = \frac{da}{dt_{\text{fatigue}}} + \frac{da}{dt_{\text{corrosion}}} \tag{2}$$

$$\frac{da}{dt_{\text{corrosion}}} = r_{\text{MD}} \cdot \frac{da}{dt_{\text{MD}}} + r_{\text{HE}} \cdot \frac{da}{dt_{\text{HE}}} \tag{3}$$

where r_{MD} and r_{HE} are the weight factors associated with crack tip MD and HE ($r_{\text{MD}} + r_{\text{HE}} = 1$). Current test results (Figs. 2, 7a, and 8a) strongly suggest that both MD and HE mechanisms act simultaneously in CFCG. However, complications arise in the decoupled quantification of MD and HE at the tip of the growing crack.

Crack propagation by MD involves ionic diffusion (of either solvating water molecules and/or aggressive anions such as chlorides) down the crack length, the rupture of the protective oxide film, followed by dissolution of the bare metal surface. The overall MD

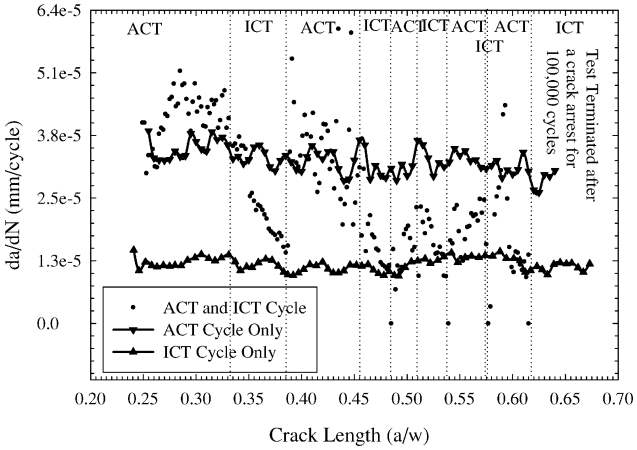

Fig. 8a Test conducted under alternating ACT and ICT environment and constant crack tip stress intensity condition.

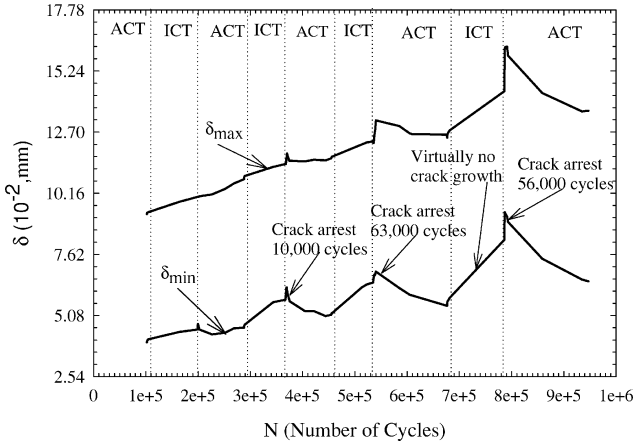

Fig. 8b Actual δ values and transition point crack arrest data obtained during an alternating ACT and ICT environment test conducted under constant ΔK.

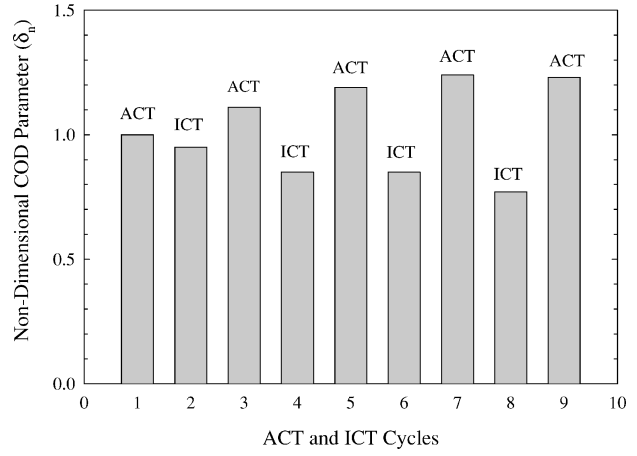

Fig. 8c Nondimensional δ_n values obtained from alternating environment test conducted under constant stress intensity condition.

assisted crack advance is given according to Faraday's law (see Ref. 9) as

$$\frac{da}{dt_{\text{MD}}} = \frac{Mi_a}{z\beta F\rho t^*}[1 - \exp(\beta t^*)] \tag{4}$$

where M is the atomic weight, ρ is the density of the metal, F is Faraday's constant, z is the number of electrons involved in the overall oxidation, β is the passivation rate parameter, and t^* is the periodicity of oxide rupture events. Application of this model requires prior knowledge of crack tip current density i_a, which is a

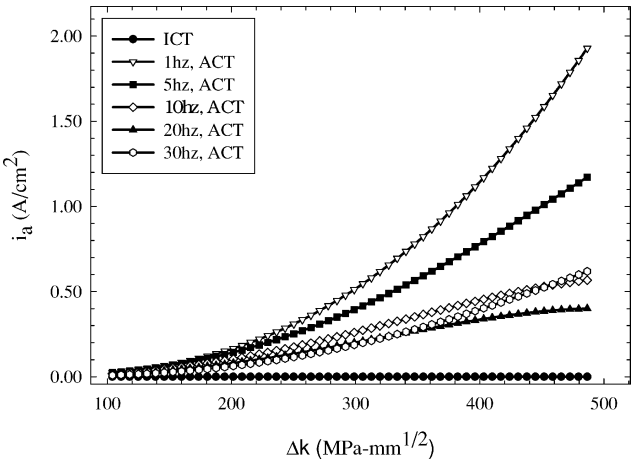

Fig. 9 Crack tip current density at various frequencies based on MD model.

measure of the corrosion rate (electrochemical process). However, because the current density at the crack tip can not be isolated from processes occurring in the area adjoining it or at other parts of the metal, it is a formidable task to quantify i_a at the tip of the growing crack. Nevertheless, if in some cases MD is the dominant corrosion CGR mechanism, that is, $r_{\mathrm{MD}} = 1$ in Eq. (3), then an indirect approach based on the difference between ACT and ICT CGR can be employed to estimate i_a. Equation (4) can then be rewritten as

$$\frac{\mathrm{d}a}{\mathrm{d}t_{\mathrm{MD}}} = \frac{\mathrm{d}a}{\mathrm{d}t_{\mathrm{ACT}}} - \frac{\mathrm{d}a}{\mathrm{d}t_{\mathrm{ICT}}} = \frac{Mi_a}{zF\rho} \tag{5}$$

where the right-hand side of Eq. (5) is obtained from Eq. (4) by assuming that the incubation time for oxide growth is larger than the periodicity of the oxide rupture events. As an example of this methodology, CGR of ICT and ACT at a loading frequency of 1 Hz are given in Fig. 2 as 2×10^{-5} cm/s and 6×10^{-5} cm/s, respectively, at $a/w = 0.6$. For 7075-T6 aluminum, $M \approx 26.98$ g/mol, $z = 3^+$, $F = 9.648 \times 10^4$ C/mol, and $\rho \approx 2.78$ g/cm^3. Solving Eq. (5) with these data yields $i_a = 1.19$ A/cm^2. The estimated values of i_a thus obtained are presented in Fig. 9 for specimens tested at various frequencies.

The estimation of i_a is presented as a methodology only because the actual CFCG model must also account for the effects of HE in its formulation. To account for HE, accurately, a detailed knowledge of solution composition and potential at the crack tip, the associated kinetics of hydrogen generation and diffusion, chemical equilibrium, and conventional crack tip electrochemical measurement is needed. However, most of this information is not readily available, rendering a large number of existing CFCG models either too simplistic and lacking in detail or too complex and somewhat subjective.[1,6,10–12] The simplest and most commonly used approach in modeling HE involves the determination of absorbed H as a function of time and distance from the surface, which can be estimated using diffusion and mass conservation equations as[15]

$$c = D_{\mathrm{H}} \nabla^2 c_i, \qquad i_{\mathrm{H}} t = \int_0^{\infty} \int_0^{2\pi} rc \, \mathrm{d}r \, \mathrm{d}\theta \tag{6}$$

where D_{H}, c_i, c, i_{H}, and r are diffusion coefficient of hydrogen, concentration of hydrogen, distribution of hydrogen concentration, rate of production of atomic hydrogen, and radial distance from the metal surface, respectively. Equations (6) have the following solution in terms of concentration of H (in a one-dimensional case):

$$c_{\mathrm{H}} = (i_{\mathrm{H}}/4\pi D_{\mathrm{H}}) Ei\left(-x^2/4D_{\mathrm{H}}t\right) \tag{7}$$

where Ei is the exponential integral error function and x is the distance from the metal surface. Equations (6) and (7) form the basis for HE-induced CGR term in Eq. (3) when combined with additional E/M information.

Mathematical models are extremely useful in design and use of materials. The brief discussion in this section sheds light on some aspects and difficulties encountered in CFCG modeling and leads to the conclusion that CFCG is a complex process and that a prerequisite for a useful modeling effort is the development of experimental techniques that would yield quantifiable and decoupled crack tip E/M information.

Conclusions

A better understanding of crack tip E/M processes is required before a reliable prediction methodology can be developed. This conclusion is based on the following observations and results.

1) Even a mildly aggressive (salt solution) environment has a detrimental effect on the lifetime of metal aircraft structures, irrespective of frequency (time of exposure) or stress level.

2) The so-called infinite life generally obtained under ICT conditions is never obtained under ACT conditions, even at extremely low stress levels and high frequencies.

3) Precorrosion and/or presence of corrosive environment at the crack tip drastically reduces crack initiation time, whereas keeping ACT during the crack propagation stage results in significant increase in CGR rate at all frequency and stress levels as compared to ICT conditions.

4) Changing the crack tip environment alters CGR quite rapidly. Severe crack arrest is observed at ICT to ACT environment transition points, especially at lower ΔK and R values. Whereas crack closure effects reduce as $\delta_{\min}$ is increased.

References

[1]Turnbull, A., "Modeling of Environment Assisted Cracking," *Corrosion Science*, Vol. 34, No. 6, 1993, pp. 921–960.

[2]Nakai, Y., and Wei, R. P., "Effects Of Frequency and Temperature on Short Fatigue Crack Growth in Aqueous Environments," *Metallurgical Transactions*, Vol. 19A, No. 3, 1988, pp. 543–548.

[3]Gnyp, P., "Phenomenological Aspects of the Influence of the Cyclic Loading Parameters on Corrosion-Fatigue Crack Growth," *Soviet Materials Science*, Vol. 20, No. 4, 1984, pp. 344–348.

[4]Gingell, A., and King, J., "The Effect of Frequency and Microstructure on Corrosion Fatigue Crack Propagation in High Strength Aluminum Alloys," *Acta Materialia*, Vol. 45, No. 9, 1997, pp. 3855–3870.

[5]Kitsunai, Y., Tanaks, M., and Yoshihisa, E., "Influence Of Residual Stresses and Loading Frequencies on Corrosion Fatigue Crack Growth Behavior of Weldments," *Metallurgical and Materials Transactions*, Vol. 29A, No. 4, 1998, pp. 1289–1298.

[6]Agarwala, V. S., "An In-Situ Experimental Study of the Mechanisms of Catastrophic Damage Phenomena," *Hydrogen Effects on Material Behavior*, edited by N. R. Moody and A. W. Thompson, The Mineral, Metals, and Materials Society, Warrendale, PA, 1990, pp. 1033–1045.

[7]Conor, P. C., "Crack Closure and Stress Corrosion Fracture Threshold in Mild Steel," *Corrosion*, Vol. 43, No. 10, 1987, pp. 614–621.

[8]Hudak, S., and Page, R., "Analysis of Oxide Wedging During Environment Assisted Crack Growth," *Corrosion*, Vol. 39, No. 7, 1983, pp. 285–290.

[9]Ford, F. P., "Corrosion Fatigue Crack Propagation in Aluminum-7% Magnesium Alloy," *Corrosion*, Vol. 35, No. 7, 1979, pp. 281–287.

[10]Parkins, R., "Stress Corrosion Cracking. Environment Induced Cracking of Metals," *Proceedings of the NACE Conference*, edited by R. Gangloff and M. Ives, NACE/Houston, 1990, pp. 1–20.

[11]Birnbaum, H., "Mechanisms of Hydrogen Related Fracture of Metals, Environment Induced Cracking of Metals," *Proceedings of the NACE Conference*, edited by R. Gangloff and M. Ives, NACE/Houston, 1990, pp. 21–30.

[12]Wei, R., and Gao, M., "Hydrogen Embrittlement and Environmentally Assisted Crack Growth," *Proceedings of the NACE Conference*, edited by R. Gangloff and M. Ives, NACE/Houston, 1990, pp. 789–816.

[13]Schijve, J., "Cumulative Damage Analysis in Aircraft Structures and Materials," *The Aeronautical Journal*, Vol. 74, June 1970, pp. 517–532.

[14]Wei, R., and Gao, M., "Reconsideration of Superposition Model for Environmentally Assisted Fatigue Crack Growth," *Metallurgical Transactions*, Vol. 16A, No. 11, 1985, pp. 2039–2050.

[15]Cherepanov, G., "On the Theory of Crack Growth Due to Hydrogen-Embrittlement," *Corrosion*, Vol. 29, No. 8, 1973, pp. 305–309.

[16]Austin, I., and Walker, E., "Quantitative Understanding of the Effects of Mechanical and Environmental Variables on Corrosion Fatigue Crack Growth Behavior," *The Influence of Environment on Fatigue*, Inst. of Mechanical Engineering, London, 1977, pp. 1–10.

[17]Shoji, T., Takahashi, H., Suzuki, M., and Kondo, T., "New Parameter for Characterizing Corrosion Fatigue Crack Growth," *Journal of Engineering Materials and Technology*, Transactions of the ASME, Vol. 103, No. 3, 1981, pp. 298–304.